Biointerphases (2012) 7:16
DOI 10.1007/s13758-011-0016-4

IN FOCUS: NANOMEDICINE - ARTICLE

# Polyethylenimine-Based Amphiphilic Core–Shell Nanoparticles: Study of Gene Delivery and Intracellular Trafficking

**Yuen Shan Siu · Lijun Li · Man Fai Leung · Kam Len Daniel Lee · Pei Li**

Received: 22 September 2011 / Accepted: 22 December 2011 / Published online: 9 February 2012


**Abstract** Amphiphilic core–shell nanoparticle, which is composed of a hydrophobic core and a branched polyethylenimine (PEI) shell, has been designed and synthesized as a novel gene delivery nanocarrier. In our previous study, we demonstrated that the core–shell nanoparticle was not only able to efficiently complex with plasmid DNA (pDNA) and protect it against enzymatic degradation, but also three times less cytotoxic, and threefold more efficient in gene transfection than branched 25 kDa PEI. This paper reports our further studies in the following three aspects: (1) the ability of the PEI-based nanoparticles to deliver gene in various mammalian cell lines; (2) intracellular distributions of the nanoparticles and their pDNA complexes in HeLa cells; and (3) incorporation of nuclear targeting agent into the nanoparticle/pDNA complexes to enhance the nuclear targeting ability. The PEI-based nanoparticles were able to transfect both human and non-human cell lines and their transfection efficiencies were cell-dependent. Within our four tested cell lines (MCF-7, BEL 7404, C6 and CHO-K1), gene transfer using PEI-based core–shell nanoparticles displayed gene expression levels comparable to, or even better than, the commercial Lipofectamine$^{TM}$ 2000. Confocal laser scanning microscopy showed that the nanoparticles and their pDNA complexes were effectively internalized into the HeLa cells. The in vitro time series experiments illustrated that both the nanoparticle/pDNA complexes and PEI-based nanoparticles were distributed in the cytoplasmic region after transfection for 10 and 60 min, respectively. Nuclear localization was also observed in both samples after transfection for 20 and 60 min, respectively. Incorporation of the high mobility group box 1 (HMGB1) protein for nuclear targeting has also been demonstrated with a simple approach: electrostatic complexation between the PEI-based nanoparticles and HMGB1. In the in vitro transfection study in MCF-7 cells, the expression level of the firefly luciferase gene encoded by the pDNA increased remarkably by up to eightfold when the HMGB1 protein was incorporated into the nanoparticle/pDNA complexes. Our results demonstrate that the PEI-based core–shell nanoparticles are promising nanocarriers for gene delivery.

## 1 Introduction

Gene therapy is a promising approach to treat a variety of genetic disorders [1, 2]. This approach is based on the introduction of functional genes (e.g. gene segments, siRNA) to alter defective gene expression, and to restore normal metabolism, cellular and physiological responses of patients [3, 4]. Up to now, the development of safe and efficient gene delivery carriers for clinical use is still a major challenge in human gene therapy. In the past two decades, viral vectors have been widely applied in clinical protocols. However, their applications are seriously hampered by safety issues (i.e. the possibility of inducing severe immune responses, and the provocation of mutagenesis) [5–7], difficulty in their mass production and limitation in gene loading capacity [5]. In the last decade, synthetic non-viral vectors have been rapidly developed because of the advancement in polymer science and nanotechnology. These non-viral vectors are considered as alternatives to overcome the adverse effects of viral vectors. Among the

This article is part of the Topical Collection "In Focus: Nanomedicine".

Y. S. Siu · L. Li · M. F. Leung · K. L. D. Lee · P. Li (✉)
Department of Applied Biology and Chemical Technology, The Hong Kong Polytechnic University, Hung Hom, Kowloon, Hong Kong, People's Republic of China
e-mail: bcpeili@polyu.edu.hk

various types of non-viral vectors, cationic polymers such as polylysine (PLL) [6, 7], polyethylenimine (PEI) [8–11], polyamidoamine dendrimer (PAMAM) [12–15] and chitosan [16–18] have received a great deal of attention owing to their advantageous properties as compared with the viral and cationic liposome-based vectors. For examples, they are easy to prepare and to be chemically modified. They also do not induce specific immune responses.

Many studies have suggested that branched PEI with an average molecular weight of 25 kDa is one of the most promising polymeric non-viral vectors because of its unique chemical and structural properties [19]. It possesses high cationic charge density, thus can effectively condense nucleic acids into nano-sized particles through strong electrostatic interaction. The resultant polyplexes can protect nucleic acids against enzymatic degradation, facilitate interaction with cell surface and enhance cellular uptake efficiency. After cellular internalization, the high amine density of PEI can assist the endosomal escape of the polyplexes from lysosomal compartments via the well-known proton sponge effect. The gene cargos are then released and expressed in a variety of mammalian cells [10]. Thus, PEI often possesses high transfection efficiency. Despite the many advantages of the PEI-based vectors, they have only achieved limited success, possibly because of their high cytotoxicity and the broad particle size distribution of the resultant polyplexes [20]. Thus considerable efforts have been made to reduce the cytotoxicity of PEI, such as modifying PEI molecules to contain poly(ethylene glycol) [21, 22], carboxylic acid group [23] and acid-degradable amino ketal branches [24]. However, these PEI modification methods usually involve multi-step syntheses and tedious purification processes. They may also alter the intrinsic properties of PEI (e.g. its sponge effect), thus resulting in a lower transfection efficiency.

To address the PEI cytotoxicity problem and enhance gene transfection efficiency, we have previously designed a novel type of amphiphilic core–shell nanoparticle that is composed of a poly(methyl methacrylate) (PMMA) core and a branched PEI shell for gene delivery [25, 26]. The PMMA–PEI nanocarrier is spherical in shape, monodisperse in aqueous medium and has a well-defined core–shell nanostructure with a highly extended PEI shell in water. The particle design is based on two main rationales: (1) to reduce PEI cytotoxicity through immobilizing the PEI molecules onto solid particles since the PEI toxicity is caused by the multiple attachment of cationic PEI onto the cell surface [27]; (2) to reduce the amount of PEI needed to form complex nanoparticles with DNA molecules through using preformed uniform core–shell nanoparticles containing PEI shells. Our previous results have demonstrated that this new type of PEI-based core–shell nanoparticles could effectively condense nucleic acids and protect them against enzymatic degradation. Most importantly, they were three times less cytotoxic than the branched PEI, and three times more efficient in transfection. Furthermore, loading plasmid DNA (pDNA) onto the uniform PMMA–PEI nanocarriers gave a much better control over size distribution than the direct complexation between PEI polymer and pDNA, thus improving the pharmacokinetic and therapeutic efficacy of the delivered nucleic acids.

As part of our continuous effort to develop this novel type of PEI-based core–shell nanocarrier, we herein report our studies on gene transfer ability of the PMMA–PEI nanocarrier in various mammalian cells and intracellular path of the nanocarrier in the HeLa cell. In addition, the targeting ability of the PMMA–PEI nanocarrier has also been demonstrated through the incorporation of the high mobility group box 1 protein (HMGB1), a nuclear targeting protein.

## 2 Experimental

### 2.1 Materials

Branched PEI with average molecular weight of 25 kDa (water-free) was obtained from Aldrich. Methyl methacrylate (Aldrich) was purified by washing three times with 10% sodium hydroxide solution and then with deionized water until the pH of the water layer dropped to 7. It was further purified by vacuum distillation. *tert*-Butyl hydroperoxide (70% solution in water) was obtained from Acros. Poly(aspartic acid) (pAsp) and fluorescein isothiocyanate (FITC) isomer 1 were purchased from Sigma-Aldrich. Luciferase Assay System and plasmid pGL3-Control vector encoding the firefly luciferase reporter gene were purchased from Promega. The plasmid was propagated in *Escherichia coli* (JM109) and was purified by QIA Spin Miniprep Kit (Qiagen). High mobility group box protein (HMGB1) was extracted and purified from pig thymus according to the methodology of Goodwin et al. [28]. Lipofectamine™ 2000, all cell culture media and sera were purchased from Invitrogen. Label IT® TM-Rhodamine Nucleic Acid Labeling Kit was purchased from Mirus.

### 2.2 Preparation and Characterization of PMMA–PEI Core–Shell Nanoparticles

The PMMA–PEI amphiphilic core–shell nanoparticles were prepared according to our previously described method [25]. After polymerization, the crude particle dispersion was purified through repeated centrifugations and decantations with de-ionized water until the conductivity of the supernatant was similar to that of the water used. Particle size and size distribution were measured on a

Coulter LS 230 Particle Size Analyzer. *zeta*-Potential of the PMMA–PEI nanoparticles were determined with a Malvern Zetasizer 3000HS (Malvern, UK) in a 1 mM NaCl aqueous solution. The nanostructures of the particles were observed with a JEM 100 CX transmission electron microscope (TEM) with an accelerating voltage of 100 kV. The dried PMMA–PEI nanoparticles on a carbon-coated grid were treated with a small drop of 2% phosphotungstic acid (PTA) for an appropriate time. The morphology of the particles was also observed with a JEOL JSM 6335F field emission scanning electron microscope (SEM). Samples were prepared by spreading a drop of dilute particle dispersion on a glass surface and dried in a dust-free environment at room temperature. The dried specimen was then coated under vacuum with a thin layer of gold to a depth of 5 Å.

### 2.3 Formation of Nanoparticle/pDNA, PEI/pDNA, pDNA/HMGB1 and Nanoparticle/pDNA/HMGB1 Complexes

pGL3-Control vector was used as the pDNA for studying the complexing abilities of various gene carriers. Nanoparticle/pDNA and PEI/pDNA complexes were prepared by mixing various amounts of nanoparticles (ranging from 0 to 800 μg) and PEI polymer (ranging from 0 to 196 μg) with 0.3 μg of pDNA, and allowed to incubate at room temperature for 30 min. The complexing ratio is expressed as the molar fraction of the amino group in PEI to the phosphate group in pDNA (N/P ratio). Besides, pDNA/HMGB1 and nanoparticle/pDNA/HMGB1 complexes were prepared by mixing 0.1 μg of HMGB1 protein with the pDNA or nanoparticle/pDNA complexes, and incubated at room temperature for 20 min. After the incubation, all complexes were analyzed by 0.8% agarose gel electrophoresis.

### 2.4 Release of pDNA from Nanoparticle/pDNA and Nanoparticle/pDNA/HMGB1 Complexes

The ability to release pDNA from the nanoparticle/pDNA and nanoparticle/pDNA/HMGB1 complexes and the integrity of the released pDNA were investigated by the addition of pAsp. The pAsp molecules were mixed with the complexes in a pAsp to pDNA molar ratio of 100. The mixture was then incubated at room temperature for 2 h and was analyzed by 0.8% agarose gel electrophoresis.

### 2.5 Cell Culture

The human cell lines HeLa, MCF-7, BEL 7404 and the non-human cell lines C6, CHO-K1 were cultured in low glucose Dulbecco's modified Eagle's medium (DMEM), supplemented with 10% (v/v) fetal bovine serum (FBS), 100 units/mL penicillin and 100 μg/mL streptomycin (P/S) at 37°C in a humidified atmosphere containing 5% $CO_2$.

### 2.6 In Vitro Transfection Study

For the transfection studies of PMMA–PEI nanoparticles and PEI polymer, cells were seeded in 6-well plates with $4 \times 10^5$ cells per well. After overnight incubation, cells were treated with nanoparticle/pDNA and PEI/pDNA complexes prepared at N/P ratios of 3, 5, 8, 10 and 15. All samples were prepared in a serum-free medium and incubated with cells for 4 h. Subsequently, medium in each well was replaced with fresh complete growth medium, and the cells were collected after incubation for another 32 h.

For the transfection study of nanoparticle/pDNA/HMGB1 complexes, cells were seeded in 24-well plates with $1.2 \times 10^5$ cells per well. They were then treated with the nanoparticle/pDNA/HMGB1 complexes for 4 h, and collected after incubation for another 20 h.

The expression level of the firefly luciferase reporter gene of the pGL3-Control plasmid was analyzed by Luciferase Assay System (Promega). Cells were collected according to the manufacturer's instruction and the relative luminescence units (RLU) were measured with a Turner Design TD-20/20 Luminometer (Promega). In all studies, Lipofectamine™ 2000 was used as a control and Lipofectamine/pDNA were prepared according to the manufacturer's instruction.

### 2.7 Intracellular Trafficking of PMMA–PEI Nanoparticles and Nanoparticle/pDNA Complexes by Confocal Laser Scanning Microscopy

The intracellular paths of the PMMA–PEI nanoparticles and their pDNA complexes were studied by the confocal laser scanning microscopy. In this study, the nanoparticles were labeled with FITC isomer 1 according to our previously described method with minor modification [29]. The nanoparticles were incubated with FITC in borate buffer (0.1 M, pH 8.5) at nanoparticle to FITC ratio of 10–1 (w/w) for 4 h at room temperature. The unreacted FITC molecules were removed by dialysis against 1 L of deionized distilled water (1,000x volume of the labeling reaction) for 16 h. For the dual fluorescent labeling experiment, the pDNA was labeled with tetramethyl-rhodamine (TM-rhodamine) according to the instruction provided with the Label IT® TM-Rhodamine Nucleic Acid Labeling Kit.

HeLa cells were seeded in 8-well chamber slides with $4 \times 10^4$ cells per well and incubated overnight. The cells were then treated with fluorescent labeled nanoparticles and nanoparticle/pDNA complexes (with N/P ratio of 5).

At various time points (10 min to 4 h), the cells were fixed with 4% (v/v) paraformaldehyde in PBS for 30 min and visualized under a confocal microscope (LSM 510 META, Carl Zeiss Inc.) with an argon laser (488 nm excitation) and a 505–530 nm band-pass filter. For the dual fluorescence images, the TM-rhodamine signal was obtained with a helium/neon laser (543 nm) and a band-pass filter of 576–640 nm.

## 3 Results and Discussion

### 3.1 Preparation and Characterization of PMMA-PEI Core–Shell Nanoparticles

The PMMA–PEI amphiphilic core–shell nanoparticles were prepared according to our previously described procedures [25]. Methyl methacrylate (MMA) monomer was polymerized with cationic branched PEI (25 kDa) in a weight ratio of 1:2. After purifying the resultant nanoparticles, the actual compositions of the nanoparticles were determined, and they contained 29% PEI and 71% PMMA. The PMMA–PEI nanoparticles displayed positive surface charges in the range of +35 to +40 mV as measured in a 1 mM of NaCl solution. The number and volume average particle diameters were 103 and 110 nm, respectively, with very narrow particle size distribution [polydispersity index ($D_v/D_n$) = 1.07]. SEM image shows that the nanoparticles were spherical and highly uniform (Fig. 1). Through selective staining of the particles with a diluted PTA solution for an appropriate time, the core–shell nanostructure of the particles was clearly revealed with the TEM (inset of Fig. 1).

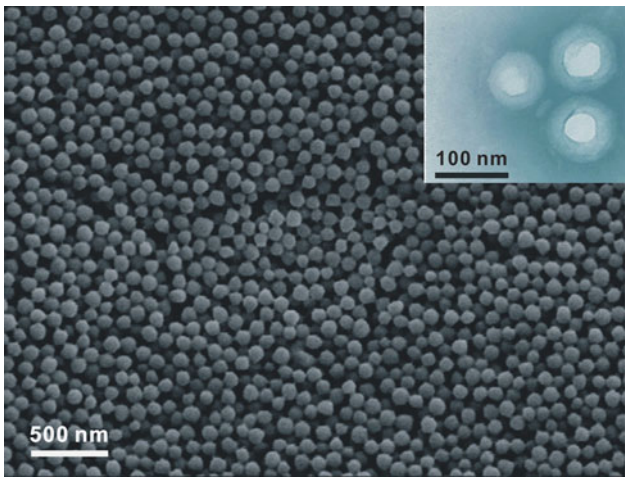


**Fig. 1** SEM micrograph of PMMA–PEI core–shell nanoparticles. *Inset* TEM micrograph of nanoparticles showing well-defined PMMA cores (*lighter part*) and PEI shells (*darker region*)

### 3.2 Performance of the Nanoparticles as pDNA Carrier

#### *3.2.1 Formation of Nanoparticle/pDNA Complexes*

DNA condensation onto the gene carrier is the first step in gene delivery. In this study, the pDNA condensation capability of our core–shell nanoparticles was compared with the branched 25 kDa PEI polymer by agarose gel electrophoresis. Figure 2 (upper panel) shows that both PMMA–PEI nanoparticles and PEI polymer could effectively condense pDNA and complete pDNA retardation occurred at the N/P ratio of 2. However, at lower N/P ratios, the PMMA–PEI nanoparticles are far more efficient than the PEI. For example, at the N/P ratio of 1, much less DNA was left uncomplexed with the nanoparticle than the PEI alone. This is shown by the much weaker intensity of the uncomplexed pDNA band from the nanoparticle-based complexation than that of PEI. These results indicate that the PMMA–PEI nanoparticles have a much better DNA complexing capability than the PEI polymer.

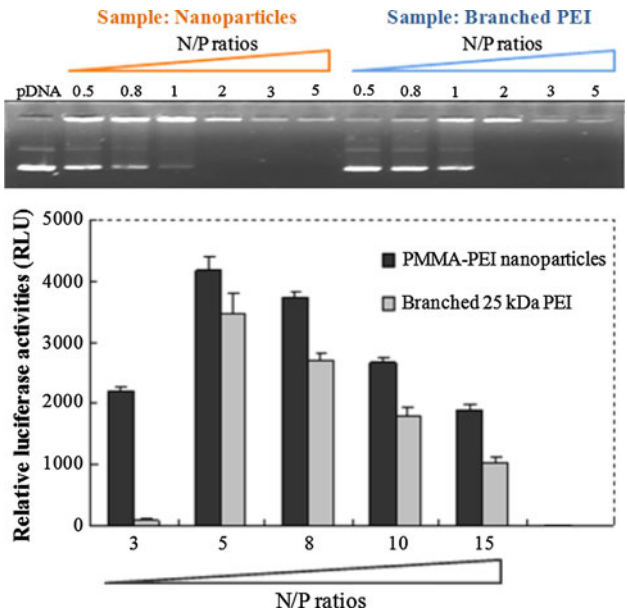


**Fig. 2** *Upper panel* Agarose gel retardation study on the formation of nanoparticle/pDNA and PEI/pDNA complexes at various N/P ratios (ranging from 0.5 to 5). *Lower panel* Comparison of PMMA–PEI nanoparticles and PEI mediated transfection at various N/P ratios in HeLa cells. 2 μg of pGL3-Control plasmid was used for the preparation of each complex, and the luciferase activities were measured 36 h after transfection

#### *3.2.2 Gene Transfection Mediated by PMMA–PEI Nanoparticles*

The pGL3-Control pDNA used to complex with the nanoparticles carries the firefly luciferase gene. The transfection efficiency can therefore be assayed by measuring the firefly luciferase activity in the target cells. In

our in vitro transfection experiment, HeLa cells were used and the transfection efficiency was determined by the firefly luciferase enzyme activity expressed in RLU.

We have tested the effect of various N/P ratios on the transfection efficiency. Since complete complexation occurred at the N/P ratio of 2, we started with the N/P ratio of 3. At this N/P ratio, the gene transfer ability of the PMMA–PEI nanoparticles was far more efficient than that of the PEI polymer (Fig. 2, lower panel). At the N/P ratio of 5, the transfection efficiency of the nanoparticle/pDNA complexes was about twice of that at the N/P ratio of 3. This is probably due to the increase in the amine content in the nanoparticle/pDNA complexes. The higher amine content provides a higher buffering capacity to facilitate the endosomal escape of the pGL3-Control plasmid into the cytoplasm. As more pDNA are in the cytoplasm, more could be transported from the cytoplasm into the nucleus for gene expression. However, further increasing the N/P ratio from 5 to 15 did not show improvement in the transfection efficiency but a decline instead. This may be due to the fact that excess positive charges on the nanoparticle/pDNA complex surface may lead to distortion of the cell membrane and cell lysis. Therefore, the optimal N/P ratio for PMMA–PEI nanoparticle mediated transfection in HeLa cells is 5 and this N/P ratio gave the best balance between the endosomolytic activity and cellular toxicity of the PEI molecules present on the surface of the nanoparticles.

In the range of N/P ratio we have tested (3–15), the PMMA–PEI nanoparticles always demonstrate a higher transfection efficiency than the branched PEI polymer. This is probably due to the fact that the PEI polymer is more toxic to the cells than the PMMA–PEI nanoparticles [26]. With more healthy viable cells present, higher firefly luciferase enzyme activity would obviously be detected. The above findings demonstrate clearly that the PMMA–PEI nanoparticle system is a much better system than the PEI polymer, at least in in vitro transfection experiments.

#### 3.2.3 *PMMA–PEI Nanoparticle Mediated Transfection in Human and Non-Human Cell Lines*

In in vitro transfection studies, the commercially available Lipofectamine™ 2000 is commonly used. In order to compare the transfection efficiency between the PMMA–PEI nanoparticles and the commercially available Lipofectamine™ 2000, another four mammalian cell lines, MCF-7, BEL 7404, C6 and CHO-K1, were used. The first two cell lines are human carcinoma cells while the other two are rat brain cells and hamster ovary cells, respectively. Results in Fig. 3 show that the PMMA–PEI nanoparticles could transfect all four cell lines and in each of these four cell lines, the optimal transfection efficiency occurred at the N/P ratio of either 5 or 8. In the MCF-7 and the CHO-K1 cells, the PMMA–PEI nanoparticles were far more efficient than the lipofectamine while in the other two cell lines, the PMMA–PEI nanoparticles were less efficient then the lipofectamine. These results show that the PMMA–PEI nanoparticles are as efficient as, if not more efficient than, the commercially available lipofectamine and they are efficient in transfecting both human and non-human mammalian cells. We therefore believe that this PEI-based nanoparticle has the potential to be used as a gene carrier in both human and non-human systems.

### 3.3 Intracellular Trafficking of PMMA–PEI Nanoparticles and Nanoparticle/pDNA Complexes

In order to better understand the mechanism of PMMA–-PEI mediated transfection, fluorescent labels and imaging techniques were used to track the intracellular paths and distributions of the nanoparticles and their pDNA complexes.

#### 3.3.1 *Intracellular Trafficking of PMMA–PEI Nanoparticles*

Confocal laser scanning microscopy was employed to track the post-transfection of FITC-labeled PMMA–PEI nanoparticles. Figure 4 shows the confocal laser scanning microscopic images of HeLa cells at various post-transfection time points. At 20 min after transfection, only very weak FITC signals were detected and the green fluorescence was just visible as silhouette. It indicates that some of the labeled PMMA–PEI nanoparticles were starting to interact with the cell surface. The fluorescence appeared as patches, suggesting that the PMMA–PEI nanoparticles were aggregating on specific areas of the plasma membrane. At 1 h after transfection, the green fluorescence signals were mainly observed in the cytoplasmic region of the HeLa cells. This indicates that the FITC-labeled nanoparticles were internalized into the cells, and some had even migrated into the nuclear region (as indicated by the arrows). After 2 h post-transfection, more and more FITC-labeled nanoparticles were found to have been taken up by the cells, and endocytotic vesicles became observable. Nucleoli in the nuclear region had also lightened up and this is a clear evidence of nuclear localization of the PMMA–PEI nanoparticles.

#### 3.3.2 *Intracellular Trafficking of Nanoparticle/pDNA Complexes*

Figure 5 shows that the PMMA–PEI nanoparticles after complexing with pDNA were internalized by the cells at a faster rate than the nanoparticles alone. At 10 min

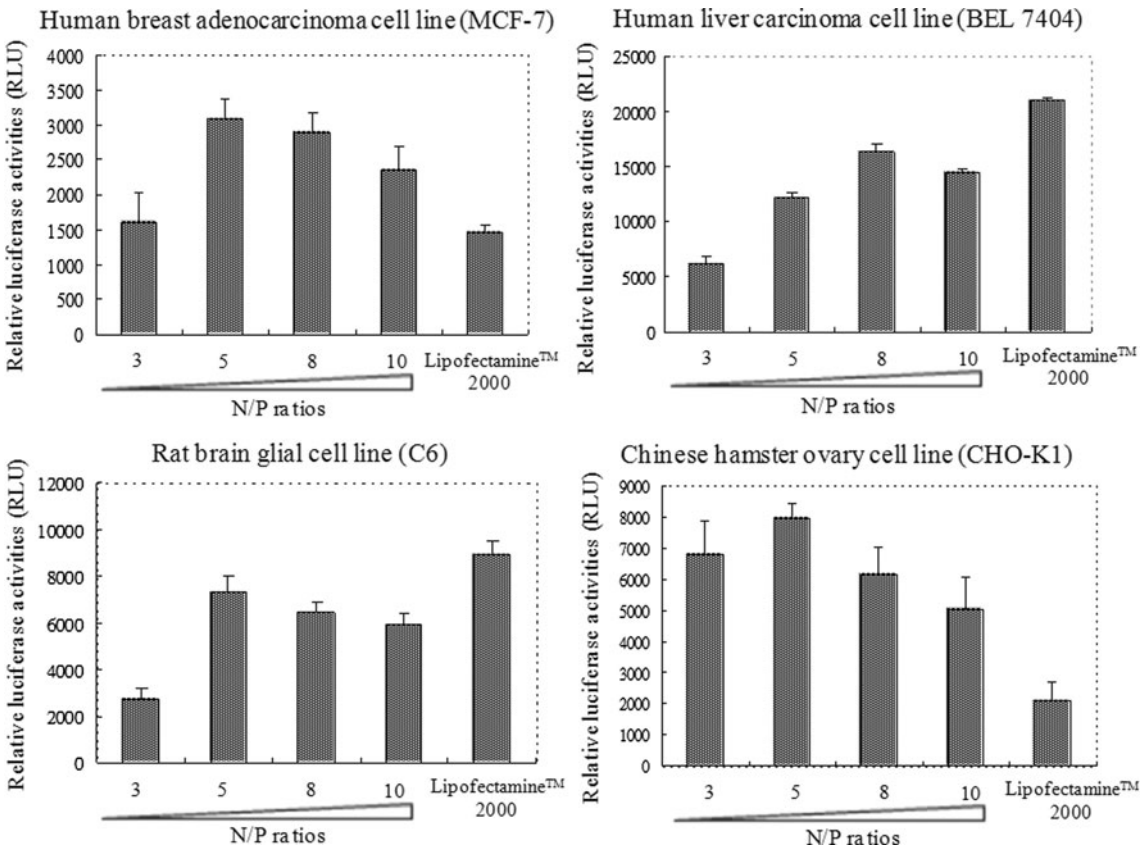


**Fig. 3** PMMA–PEI nanoparticle mediated transfection in human breast adenocarcinoma cell line (MCF-7), human liver carcinoma cell line (BEL 7404), rat brain glial cell line (C6) and Chinese hamster ovary cell line (CHO-K1). 2 μg of pGL3-Control plasmid was used for the preparation of each complex, and the luciferase activity was measured 36 h after transfection

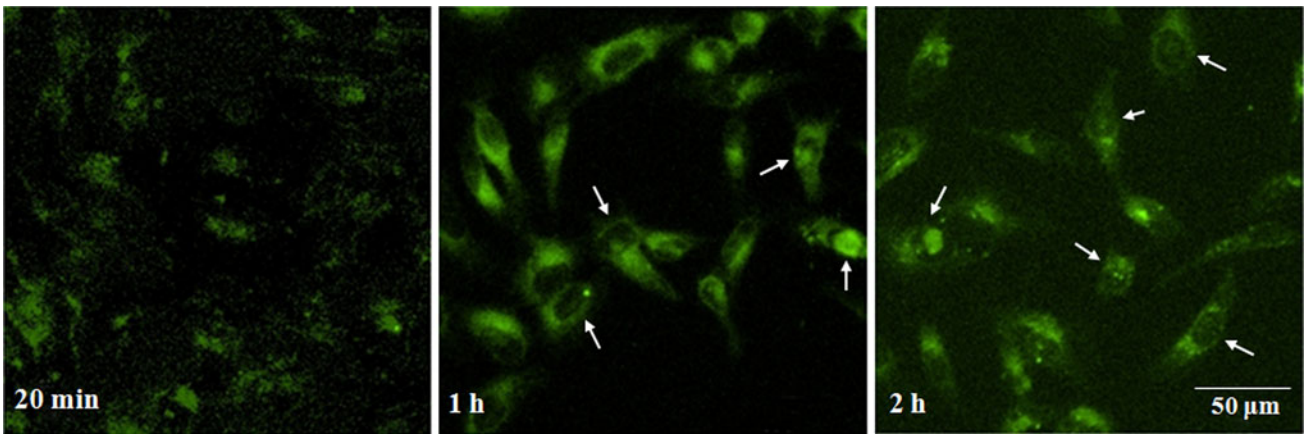


**Fig. 4** Cellular internalization and nuclear localization of FITC-labeled PMMA–PEI nanoparticles in HeLa cells. Cells were incubated with the nanoparticles for 20 min, 1 h and 2 h, respectively. Cells with nuclear fluorescence are indicated by the *arrows*

post-transfection, green fluorescence signals were already observable in the cytoplasm of HeLa cells. From 10 to 40 min, higher and higher fluorescence intensities were observed inside the cells, indicating the presence of increasing FITC-labeled nanoparticle/pDNA complexes in the HeLa cells. At the same time, the first evidence of fluorescence inside the nucleus was observed at 20 min after transfection. Cell population with nuclear fluorescence had further increased at 40, 50 and 60 min. After 4 h post-transfection, the FITC-labeled nanoparticle/pDNA complexes were observable in both the cytoplasmic and nuclear regions in most of the cells. Further study by using

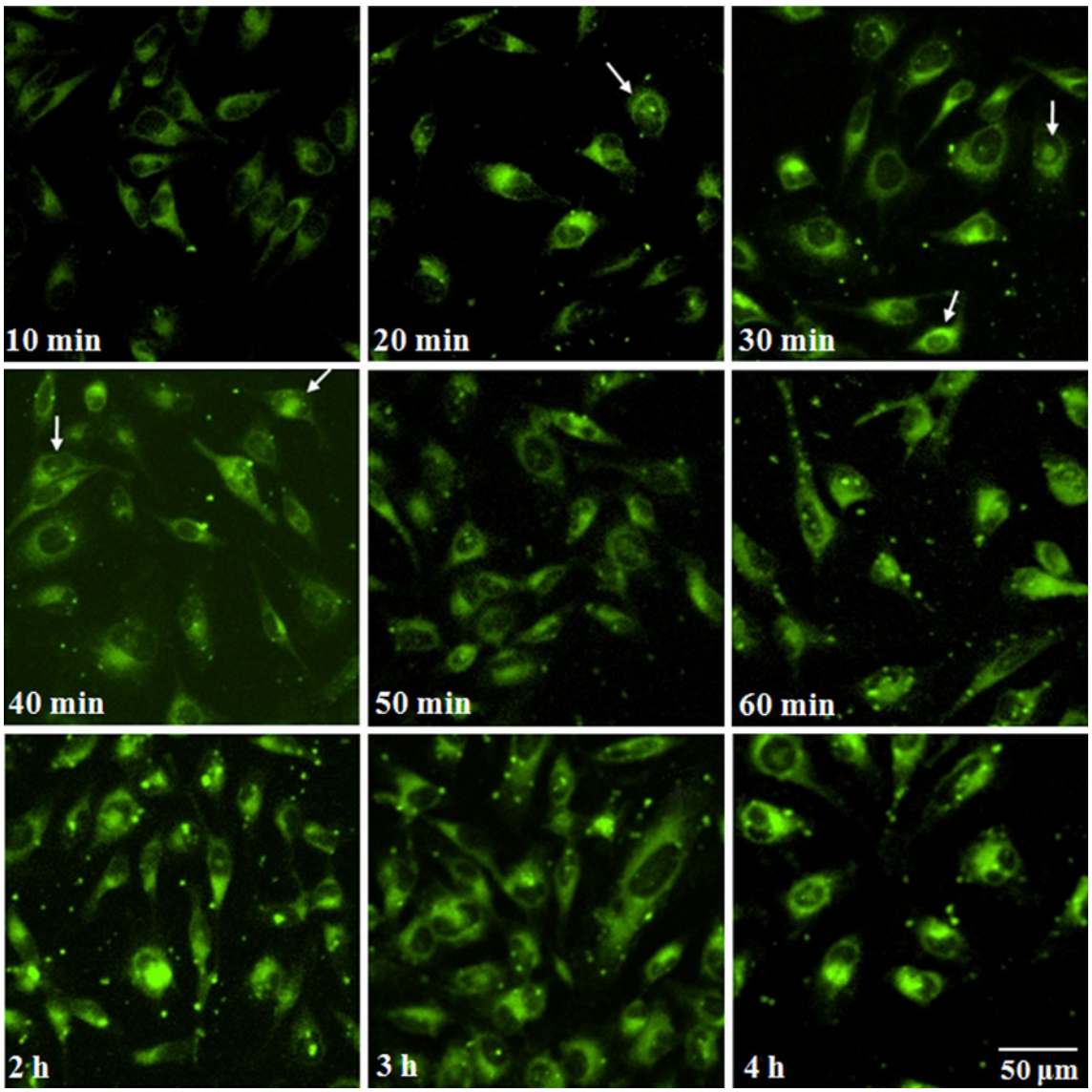


**Fig. 5** Cellular internalization and nuclear localization of FITC-labeled nanoparticle/pDNA complexes in HeLa cells. Cells were incubated with the complexes for 10 min to 4 h. Cells with nuclear fluorescence (indicated by *arrows*) were observed at 10–40 min. After 50 min of incubation, most of the cells exhibited nuclear accumulation of the FITC-labeled complexes

dual-fluorescent labeling, in which the pDNA was labeled with TM-rhodamine, confirmed that the pDNA remained bound to the nanoparticle even at 4 h post-transfection. The confocal laser micrograph is shown in Fig. 6. All these results suggest that the cellular internalization and nuclear localization rates of the PMMA–PEI nanoparticles are actually enhanced with the association of the pDNA. This may attribute to the fact that the nanoparticle/pDNA complexes have a smaller diameter than the PMMA–PEI nanoparticles as a result of electrostatic neutralization between the negatively charged pDNA and the positively charged PEI shell. This effect has been demonstrated in our previous study [26]. For example, at the N/P ratio of 5, the complexed nanoparticles have a reduction in their diameters from 146 to 124 nm. We believe that the smaller particle size of the complexes is the key factor in the increase in the cellular internalization and the nuclear localization efficiency.

### 3.4 Nanoparticle/pDNA Complexes Containing Nuclear Targeting Protein

For non-viral gene delivery carriers, the nuclear membrane is actually the major barrier for efficient gene transfer. Quantitative cytoplasmic microinjection studies have demonstrated that only 0.1% of the naked pDNA could reach the nucleus where the transgene is transcribed and subsequently expressed [30]. Even for the well studied

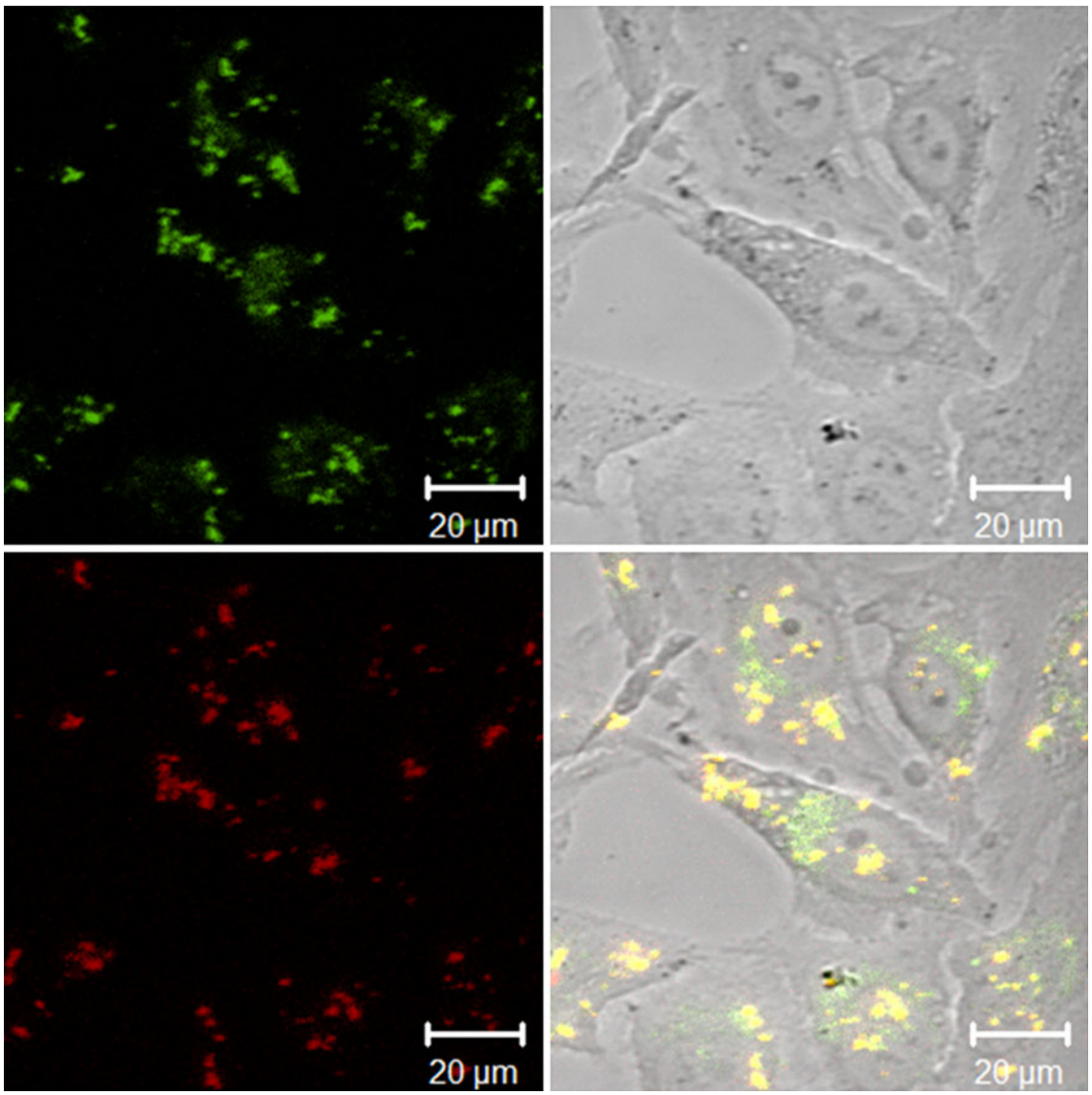


**Fig. 6** Confocal laser scanning microscopic image of HeLa cells after 4 h post-transfection with dual-fluorescent labeled nanoparticle/pDNA complexes. The *red signals* (pDNA) were all co-localized with the *green signals* (PMMA–PEI), indicating the presence of pDNA with the nanoparticles

PEI/pDNA polyplexes, which show nuclear accumulation property, only 1% of the pDNA can be transported into the nucleus [31]. In order to overcome the nuclear membrane barrier and to further improve the PMMA–PEI nanoparticle gene delivery system, the nuclear protein, HMGB1 was combined with the nanoparticle/pDNA complex.

### *3.4.1 Incorporation of Nuclear Protein into the Nanoparticle/pDNA Complex*

In this part of study, the nuclear protein HMGB1 was added as an additional component in the existing nanoparticle/pDNA gene delivery system. The nuclear protein HMGB1 contains two homologous DNA binding motifs (HMG box A and B) and a polyacidic tail [32]. It also contains two nuclear localization signals (NLSs) for controlled nuclear transport [33, 34]. The rationale for our design is to use the HMGB1 protein as a nuclear targeting agent. Being an ampholyte, the HMGB1 protein has the ability to interact with both the negatively charged pDNA and the positively charged PMMA–PEI nanoparticle simply by electrostatic interaction. Introduction of HMGB1 to the nanoparticle/pDNA complexes can result in the formation of nanoparticle/pDNA/HMGB1 complexes through interaction between the amine group of the PEI shell and the terminal acidic domain of the HMGB1 protein. The

resultant nanoparticle/pDNA/HMGB1 complexes should have the NLSs present on the surface of the complex to facilitate the nuclear import process.

We have shown that the presence of the HMGB1 protein does not affect the complexing capability of the PMMA–PEI nanoparticles. With (Fig. 7, left panel, lane 5) or without the inclusion of HMGB1 (lane 2), pDNA molecules were completely complexed to the PMMA–PEI nanoparticles at the N/P ratio of 5. Furthermore, all the pDNA were released from the nanoparticle/pDNA/HMGB1 complexes when incubated with pAsp in a pAsp/pDNA molar ratio of 100. The released pDNA remained intact in the supercoiled form (lane 6). It indicates that the inclusion of HMGB1 in the nanoparticle gene delivery system does not affect the integrity of the DNA nor the ability of the system to release the complexed DNA.

It was also found that the pDNA released from the nanoparticle/pDNA/HMGB1 complexes displayed a slower electrophoretic mobility than the naked pDNA (lane 1), and the pDNA released from the nanoparticle/pDNA complexes (lane 3), but similar to that of the pDNA/HMGB1 complexes (lane 4). This finding is actually reasonable as HMGB1 is a well known DNA binding chromosomal protein and it is expected to bind the pDNA even when the pDNA is released from the PMMA–PEI nanoparticle. The results suggest that the pDNA may still retain its nuclear targeting ability by HMGB1 binding even if the nanoparticle is disassembled during the gene transfer process. The binding effect may help to shuttle the exogenous gene into the nucleus for gene expression.

### 3.4.2 *Transfection Efficiency of the Nanoparticle/pDNA/HMGB1 Complexes*

The effectiveness of including HMGB1 in the PMMA–PEI nanoparticle gene delivery system was investigated by in vitro transfection of MCF-7 cells. The nanoparticle/pDNA/HMGB1 complexes were prepared at various N/P ratios, but with a fixed pDNA/HMGB1 weight ratio of 3, based on the optimal ratio reported by Kato et al. [35] and Namiki et al. [36] in their in vitro and in vivo liposome mediated transfection studies. For comparison, same N/P ratios of nanoparticle/pDNA complexes with and without HMGB1 were studied. Lipofectamine™ 2000 and pDNA/HMGB1 complexes were used as controls. Four N/P ratios of 2, 5, 8 and 10 were tested and it was found that in all four ratios, much higher luciferase activities were observed with the inclusion of HMGB1 (Fig. 7, right panel). These results indicate that HMGB1 can significantly enhance the efficiency of the PMMA–PEI nanoparticle gene delivery system. The most remarkable result was observed at the N/P ratio of 5 in which the system has its highest transfection efficiency and it was more than eightfold higher than that of just the PMMA–PEI nanoparticles. It is known that the HMGB1 protein binds to the RAGE (receptor for advanced glycation endproducts) presented on the cell surface [37] and has NLSs [33]. Therefore, it is reasonable to suggest that with the inclusion of HMGB1 on the nanoparticle/pDNA complex, cellular uptake is facilitated via ligand–receptor interaction and nuclear localization is enhanced via the NLS.

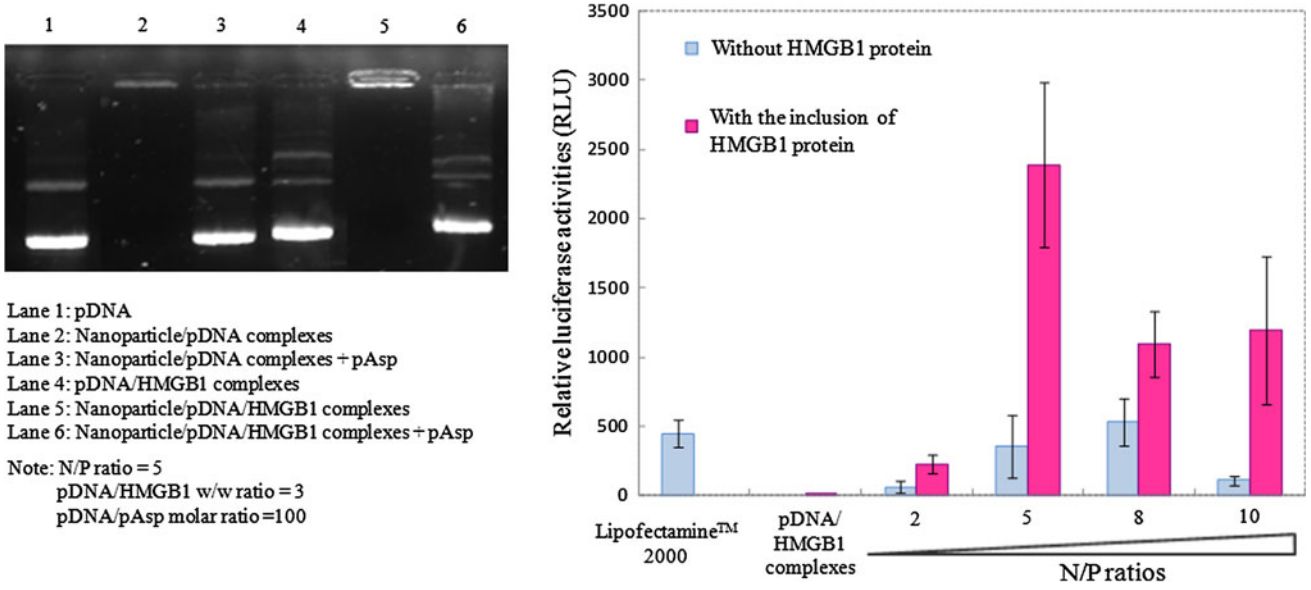


**Fig. 7** *Left panel* Agarose gel analysis for the formation of complexes at the N/P ratio of 5, and the release of pDNA from complexes using pAsp at a pAsp/pDNA molar ratio of 100. *Right panel* Transfection efficiencies of nanoparticle/pDNA/HMGB1 complexes and nanoparticle/pDNA complexes at various N/P ratios in MCF-7 cells. 0.4 μg of pGL3-Control plasmid was used for the preparation of each complex, and the luciferase activities were measured 24 h after transfection

## 4 Summary and Conclusions

This work described the use of amphiphilic core–shell nanoparticle consisting of poly(methyl methacrylate) core with branched PEI shell as a versatile gene carrier. Results based on the agarose gel retardation assay and in vitro transfection study showed that our PMMA–PEI core–shell nanoparticle has a better DNA condensation capacity and higher gene transfer efficiency than the branched 25 kDa PEI. The in vitro transfection experiments also suggested that the PMMA–PEI nanoparticles could be used in transfection of both human and non-human cells (e.g. MCF-7, BEL 7404, C6 and CHO-K1), and their gene expression levels were higher than, or at least comparable to the commercially available transfection agent, Lipofectamine$^{TM}$ 2000. Confocal laser scanning microscopy illustrated that the PMMA–PEI nanoparticle and its pDNA complexes were effectively internalized by HeLa cells, and eventually localized in the nuclear region of the cells. The inclusion of nuclear targeting agent, HMGB1 protein with the nanoparticle/pDNA complexes significantly enhanced the foreign gene expression by up to eightfold. As the PMMA–PEI nanoparticle can effectively transfect different cell lines and can be modified with targeting agent, this PEI-based amphiphilic core–shell nanoparticle is an efficient and versatile nanocarrier for gene delivery.

**Acknowledgments** We gratefully acknowledge The Hong Kong Polytechnic University, the University Research Grants Council of Hong Kong SAR (Project No. Poly 5283/02P), and The Lo Ka Chung Centre for Natural Anti-Cancer Drug Development for their financial support of this research.



## References

1. Liu F, Huang L (2002) J Control Release 78:259
2. Lundstrom K, Boulikas T (2003) Technol Cancer Res Treat 2:471
3. Segura T, Shea LD (2001) Annu Rev Mater Res 31:25
4. Thomas M, Klibanov AM (2003) Appl Microbiol Biotechnol 62:27
5. Kay MA, Liu D, Hoogerbrugge PM (1997) Proc Natl Acad Sci 94:12744
6. Jeon E, Kim H-D, Kim J-S (2003) J Biomed Mater Res Part A 66A:854
7. Cho KC, Kim SH, Jeong JH, Park TG (2005) Macromol Biosci 5:512
8. Lungwitz U, Breunig M, Blunk T, Göpferich A (2005) Eur J Pharm Biopharm 60:247
9. Günther M, Lipka J, Malek A, Gutsch D, Kreyling W, Aigner A (2011) Eur J Pharm Biopharm 77:438
10. Godbey WT, Wu KK, Mikos AG (1999) J Control Release 60:149
11. Wang C-F, Lin Y-X, Jiang T, He F, Zhuo R-X (2009) Biomaterials 30:4824
12. Kitchens KM, El-Sayed MEH, Ghandehari H (2005) Adv Drug Deliv Rev 57:2163
13. Zhang X-Q, Wang X-L, Huang S-W, Zhuo R-X, Liu Z-L, Mao H-Q, Leong KW (2005) Biomacromolecules 6:341
14. Navarro G, Tros de Ilarduya C (2009) Nanomed Nanotechnol Biol Med 5:287
15. Marvaniya H, Parikh PK, Patel VR, Modi KN, Sen DJ (2010) J Chem Pharm Res 2:97
16. Mao S, Sun W, Kissel T (2010) Adv Drug Deliv Rev 62:12
17. Lavertu M, Methot S, Tran-Khanh N, Buschmann MD (2006) Biomaterials 27:4815
18. Strand SP, Lelu S, Reitan NK, de Lange Davies C, Artursson P, Vårum KM (2010) Biomaterials 31:975
19. Neu M, Fischer D, Kissel T (2005) J Gene Med 7:992
20. Kunath K, von Harpe A, Fischer D, Petersen H, Bickel U, Voigt K, Kissel T (2003) J Control Release 89:113
21. Petersen H, Fechner PM, Fischer D, Kissel T (2002) Macromolecules 35:6867
22. Zhang X, Pan SR, Hu HM, Wu GF, Feng M, Zhang W, Lu X (2008) J Biomed Mater Res Part A 84A:795
23. Zintchenko A, Philipp A, Dehshahri A, Wagner E (2008) Bioconjug Chem 19:1448
24. Shim MS, Kwon YJ (2009) Bioconjug Chem 20:488
25. Li P, Zhu J, Sunintaboon P, Harris FW (2002) Langmuir 18:8641
26. Zhu J, Tang A, Law LP, Feng M, Ho KM, Lee DKL, Harris FW, Li P (2005) Bioconjug Chem 16:139
27. Choksakulnimitr S, Masuda S, Tokuda H, Takakura Y, Hashida M (1995) J Control Release 34:233
28. Goodwin GH, Nicolas RH, Johns EW (1975) Biochim Biophys Acta 405:280
29. Feng M, Li P (2007) J Biomed Mater Res Part A 80A:184
30. Mirzayans R, Aubin RA, Paterson MC (1992) Mutat Res 281:115
31. Pollard H, Remy J-S, Loussouarn G, Demolombe S, Behr J-P, Escande D (1998) J Biol Chem 273:7507
32. Bustin M, Lehn DA, Landsman D (1990) Biochim Biophys Acta 1049:231
33. Youn JH, Shin JS (2006) J Immunol 177:7889
34. Bonaldi T, Talamo F, Scaffidi P, Ferrera D, Porto A, Bachi A, Rubartelli A, Agresti A, Bianchi ME (2003) Eur Mol Biol Organ J 22:5551
35. Kato K, Nakanishi M, Kaneda Y, Uchida T, Okada Y (1991) J Biol Chem 266:3361
36. Namiki Y, Takahashi T, Ohno T (1998) Gene Ther 5:240
37. Degryse B, Bonaldi T, Scaffidi P, Müller S, Resnati M, Sanvito F, Arrigoni G, Bianchib ME (2001) J Cell Biol 152:1197